Femtosecond laser direct inscription of mid-IR transmitting waveguides in BGG glasses

Jean-Philippe Bérubé, Arthur Le Camus, Sandra Helena Messaddeq, Yannick Petit, Younès Messaddeq, Lionel Canioni, Réal Vallée

Research Article | Vol. 7, No. 9 | 1 Sept 2017 | OPTICAL MATERIALS EXPRESS 3124
Optical Materials EXPRESS

Femtosecond laser direct inscription of mid-IR transmitting waveguides in BGG glasses

JEAN-PHILIPPE BÉRUBÉ,[1,*] ARTHUR LE CAMUS,[1,2] SANDRA HELENA MESSADDEQ,[1] YANNICK PETIT,[2,3] YOUNÈS MESSADDEQ,[1] LIONEL CANIONI,[2] AND RÉAL VALLÉE[1]

[1]*Centre d'optique, photonique et laser (COPL) – 2375 rue de la Terrasse, Université Laval, Québec G1V 0A6, Canada*
[2]*Université de Bordeaux, CNRS, CEA, CELIA, UMR 5107, F-33405 Talence, France*
[3]*Université de Bordeaux, CNRS, ICMCB, UPR 9048, F-33608 Pessac, France*
**jean-philippe.berube.2@ulaval.ca*

Abstract: A detailed investigation of the photo-inscription of waveguides in barium gallo-germanate (BGG, BaO, GeO_2, Ga_2O_3) glass is presented. Upon irradiation of BGG glass samples of different contents of germanium dioxide with a femtosecond laser pulse train, positive refractive index changes are produced over a wide range of exposure conditions. Waveguides with a controllable diameter ranging from 4 to 35 µm and a maximum index change up to 10^{-2} were inscribed. A glass sample with custom molecular composition was purified to remove hydroxyl ions and reduce the strong absorption band near 3 µm. A careful tailoring of the writing conditions allowed for the inscription of low-loss waveguides supporting only two transverse modes at the wavelength of 2.78 µm. An upper bound for the propagation losses of 0.5 ± 0.1 dB/cm was determined, showing the great potential of the BGG glass family for the fabrication of core waveguides operating in the 2-4 µm spectral range. Our results actually open a pathway towards the integration of mid-IR photonic devices based on the BGG glass family.

OCIS codes: (130.2755) Glass waveguides; (350.3390) Laser materials processing; (260.3060) Infrared.

References and links

1. T. Meany, M. Gräfe, R. Heilmann, A. Perez-Leija, S. Gross, M. J. Steel, M. J. Withford, and A. Szameit, "Laser written circuits for quantum photonics," Laser Photonics Rev. **9**(4), 363–384 (2015).
2. S. Eaton, M. Ng, R. Osellame, and P. Herman, "High refractive index contrast in fused silica waveguides by tightly focused, high-repetition rate femtosecond laser, " J. Non-Cryst. Sol. **357**(11), 2387–2391 (2011).
3. N. Riesen, S. Gross, J. D. Love, and M. J. Withford, "Femtosecond direct-written integrated mode couplers," Opt. Express **22**(24), 29855–29861 (2014).
4. R. W. Waynant, I. Ilev, and I. Gannot, "Mid-infrared laser applications in medecine and biology," Phil. Trans. R. Soc. Lond. A **351**(1780), 635-644(2014).
5. R. Muda, E. Lewis, S. O'Keeffe, G. Dooly, and J. Clifford, "Detection of high level carbon dioxide emissions using a compact optical fibre based mid-infrared sensor system for applications in environmental pollution monitoring," J. Phys. Conf. Ser. **178**(1), 012008 (2009).
6. A. Arriola, S. Gross, M. Ams, T. Gretzinger, D. Le Coq, R. Wang, H. Ebendorff-Heidepriem, J. Sanghera, S. Bayya, L. Shaw, M. Ireland, P. Tuthill, and M. Withford, "Mid-infrared astrophotonics: study of ultrafast laser induced index change in compatible materials," Opt. Mater. Express **7**(3), 698 (2017).
7. F. Chen and J. Vazquez de Aldana, "Optical waveguides in crystalline dielectric materials produced by femtosecond-laser micromachining," Laser Photonics Rev. **8**(2), 251–275 (2014).
8. J. P. Bérubé, S. H. Messaddeq, I. Skripachev, R. Vallée, and Y. Messaddeq, "The influence of sulfur content on the photosensitivity of GeS_x binary glass to infrared femtosecond pulses," Opt. Express **22**(23), 26103–26116 (2014).
9. S. Gross, N. Jovanovic, A. Sharp, M. Ireland, J. Lawrence, and M. J. Withford, "Low loss mid-infrared ZBLAN waveguides for future astronomical applications," Opt. Express **23**(6), 7946–7956 (2015).
10. J. Bai, X. Long, X. Liu, G. Huo, W. Zhao, R. Stoian, R. Hui, and G. Cheng, "Embedded optical waveguides fabricated in SF10 glass by low-repetition-rate ultrafast laser," Appl. Opt. **52**(30), 7288–7294 (2013).
11. S. S. Bayya, G. D. Chin, J. S. Sanghera, and I. D. Aggarwal, "Germanate glass as a window for high energy laser systems," Opt. Express **14**(24), 11687–11693 (2006).

#298098 https://doi.org/10.1364/OME.7.003124
Journal © 2017 Received 26 Jun 2017; revised 29 Jul 2017; accepted 31 Jul 2017; published 7 Aug 2017

Optical Materials EXPRESS

12. S. Bayya, J. Sanghera, and I. Aggarwal, "Optical transmission of BGG glass material," United States Patent 0159289A1, 21 July 2005.
13. B. McMillen, B. Zhang, K. P. Chen, A. Benayas, and D. Jaque, "Ultrafast laser fabrication of low-loss waveguides in chalcogenide glass with 0.65 dB/cm loss," Opt. Lett. **37**(9), 1418–1420 (2012).
14. R. Osellame, S. Taccheo, M. Marangoni, R. Ramponi, P. Laporta, D. Polli, S. De Silvestri, and G. Cerullo, "Femtosecond writing of active optical waveguides with astigmatically shaped beams," J. Opt. Soc. Am. B **20**(7), 1559–1567 (2003).
15. S. Velghe, J. Primot, N. Guérineau, M. Cohen, and B. Wattellier, "Wave-front reconstruction from multidirectional phase derivatives generated by multilateral shearing interferometers," Opt. Lett. **30**(3), 245–247 (2005).
16. D. Faucher, M. Bernier, G. Androz, N. Caron, and R. Vallée, "20 W passively cooled single-mode all-fiber laser at 2.8 μm," Opt. Lett. **36**(7), 1104–1106 (2011).
17. B. Poumellec, M. Lancry, A. Chahid-Erraji, and P. Kazansky, "Modification thresholds in femtosecond laser processing of pure silica: review of dependencies on laser parameters," Opt. Mater. Express **1**(4), 766–782 (2011).
18. C. Schaffer, J. Garcia, and E. Mazur, "Bulk heating of transparent materials using a high repetition rate femtosecond laser," Appl. Phys., A Mater. Sci. Process. **76**(3), 351–354 (2003).
19. J. P. Bérubé, M. Bernier, and R. Vallée, "Femtosecond laser-induced refractive index modifications in fluoride glass," Opt. Mater. Express **3**(5), 598–611 (2013).
20. S. H. Messaddeq, J. P. Bérubé, M. Bernier, I. Skripachev, R. Vallée, and Y. Messaddeq, "Study of the photosensitivity of GeS binary glasses to 800 nm femtosecond pulses," Opt. Express **20**(3), 2824–2831 (2012).
21. S. M. Eaton, H. Zhang, M. L. Ng, J. Li, W. J. Chen, S. Ho, and P. R. Herman, "Transition from thermal diffusion to heat accumulation in high repetition rate femtosecond laser writing of buried optical waveguides," Opt. Express **16**(13), 9443–9458 (2008).

1. Introduction

Over the last two decades, femtosecond laser direct inscription evolved into a compelling tool for the fabrication of tridimensional photonic devices embedded in optical materials. Recently, leading edge devices such as quantum photonic circuits [1] were successfully implemented in millimetre-scale glass chips using this technique. The performance of integrated photonic devices is directly linked to the optical characteristics of the photo-induced waveguides and the physical properties of the glassy material used as the host. An ideal host would be chemically and mechanically resistant, exhibit a relatively high glass transition temperature (T_g), present a high transmission at the wavelength of operation and yield a strong, smooth refractive index increase when irradiated with femtosecond pulses. To date, only very few glasses have shown to possess all prerequisites for the integration of high quality photo-induced devices. In fact, the complete set of properties is almost exclusive to silicate-based glasses such as fused silica [2] and borosilicates [3]. While these materials are low-cost and readily available, their optical transmission is limited to $\lambda \leq 2.2$ μm (@ $\alpha \leq$ 1dB/m) and therefore to the near-infrared spectral region.

Lately, there has been a strong incentive to develop photonic components that operate in the mid-IR spectra for applications in biology and medicine [4] and environmental monitoring [5] to name only a few. Accordingly, a recent study has been devoted to femtosecond laser inscription of waveguides in optical materials known for their optical transmission in the mid-IR [6]. Other previous studies were carried out using crystalline materials [7] but also with multicomponent glasses such as chalcogenide (ChG) [8] and fluoride glasses [9]. In most cases however, the optical characteristics of the waveguides and the material properties fall short or come with serious trade-offs. Since the lattice of crystals are compact, the absorption of femtosecond pulses leads to a decrease of the material density and hence of the refractive index [7]. As such, waveguiding structures formed in crystals are either SIW (stress induced waveguides) or DCW (depressed clad waveguides). While they are functional, these waveguides exhibit moderate (0.5 – 1 dB/cm) to high propagation losses (> 1dB/cm) and are prone to curvature losses which limit their potential integration in photonic circuits. On the other hand, waveguides relying on a positive index contrast (core waveguides) inscribed in multicomponent glasses generally present a low index contrast ($< 1 \times 10^{-3}$) and relatively high propagation losses. The sole exception being the DCW waveguides inscribed in ZBLAN by Gross et al. [9] who reported propagation losses of 0.3 dB/cm measured at $\lambda = 4$ μm.

Optical Materials EXPRESS

Among the other potential optical materials, heavy metal oxide (HMO) glasses represent attractive hosts for mid-IR photonic devices as they are mechanically resistant, chemically stable and exhibit an extended transmission in the infrared spectra up to 7-8 μm. To date, the photosensitivity to fs pulses of only a few HMO glasses has been studied [10] and the direct inscription of low-loss (< 0.5 dB/cm) single mode waveguides operating at a wavelength higher than 1.03 μm has yet to be made. Among the HMO glasses, the germanate family forms an intriguing group whose response to femtosecond laser pulses has been, to the best our knowledge, left unexplored. Owing to the photosensitivity enhancing properties of germanium, GeO_2 based glasses should allow for the formation of waveguides with a high index contrast.

Among the large family of glasses with a germanium content, a novel Barium Gallo-Germanate (BGG) glass used as an output window for high energy mid-IR lasers was reported [11]. BGG glasses are particularly interesting as they exhibit exceptional mechanical properties, are chemically stable, non-toxic, unaffected by water and low cost. In particular, the nominal composition of BGG glass as defined in Ref [11]. (12.5 BaO, 75 GeO_2, 12.5 Ga_2O_3) is stable and presents all the aforementioned properties. Furthermore, a purification method was applied to expel hydroxyl (OH-) impurities and produce BGG glasses with a high transparency extending up to λ ~5 μm [12], thus making it an interesting candidate for the inscription of integrated mid-IR photonic devices.

In this paper, we report on the inscription of low-loss waveguides in BGG glasses. First, we studied the photosensitivity of nominal BGG glass to femtosecond laser pulses. Next, we examined the influence of the molecular percentage of Germanium dioxide in the glass on the material photosensitivity. Glass samples with different GeO_2 content (while maintaining a 1:1 ratio of Ga_2O_3 and BaO) were fabricated and subsequently irradiated. Then, a halogen component was introduced during the fabrication of a BGG sample with a custom composition (17.5 BaO, 65 GeO_2, 17.5 Ga_2O_3) to eliminate bound hydroxyl in the glass matrix and suppress the strong absorption band between λ = 2.8 and 3.2 μm. Using this sample, we succeeded in inscribing low-loss core waveguides operating at a wavelength of λ = 2.785 μm. An upper bound of ≤ 0.5 ± 0.1 dB/cm was determined for the propagation losses exhibited by the waveguides. This value is slightly inferior to the best result (0.65 dB/cm) obtained by McMillen et al. for mid-IR waveguides inscribed in a GaLaS glass [13]. Our results clearly demonstrate the potential of BGG glasses as hosts for photo-induced integrated mid-IR photonic devices.

2. Experimental method

Germanate glasses based on (85-x)GeO_2, (7.5 + y)Ga_2O_3, (7.5 + y)BaO with $0 \le x \le 20$ and $0 \le y \le 12.5$ were prepared by the conventional melting-quenching technique, using 4N pure Ga_2O_3 and GeO_2 and reagent grade $BaCO_3$. $BaCO_3$, which is available in higher purity than BaO, decomposes to BaO at elevated temperatures. As BGG forms stable glasses over a broad range of compositions, glass samples were prepared while retaining the ratio Ga_20_3 / BaO = 1 (i.e. x = 2y) and varying the content of GeO_2 (from 60 to 85% molar weight). Batches of 10 g were melted at 1500 °C for 30 min in a Pt-Au crucible using an electric furnace. Subsequently, the glass melt was poured in a preheated rectangular steel mold and annealed at 30 °C below the glass transition temperature T_g (between 600 to 635 °C, depending on the Ge content). It was held isothermally for 6 hours followed by a slow cooling at a rate of 1 K/min to room temperature.

BGG glass samples generally exhibit limited infrared transparency due to the presence of hydroxyl (OH-) impurities. To reduce the concentration of OH impurities, we used a method which consists of adding a halogen component during glass preparation [12]. The halogen compound scavenges water and produces volatile halides which escape from the melted mixture. We thus replaced all the $BaCO_3$ powder previously used in the first BGG glass samples by BaF_2 powder, keeping the same molar ratio of Barium. The powders were mixed

Optical Materials EXPRESS

into a Pt-Au crucible and melted at a temperature of 1300°C during 30 min. The liquid was then quickly cooled at room temperature by casting it on a metal plate. The solid glass was heated at a temperature of 565°C, slightly below the T_g near 580°C, during 5 hours, to release the stresses. The sample will be referred to as BGG-BaF for the remainder of the manuscript. Finally, the glass samples were cut to form 4 mm thick planar samples (15 x 20 mm^2) and faces were polished.

The transmission spectra of the samples were measured at room temperature in the 3–15 µm spectral range with a spectral resolution of 2.0 cm^{-1} using a FT-IR spectrometer (Perkin Elmer, Frontier). The glasses present good optical quality and similar transmission spectra which extend up to λ = 5 µm. The spectra of BGG-65 (17.5 BaO, 65 GeO_2, 17.5 Ga_2O_3) and BGG-BaF in the mid-IR range are presented in Fig. 1.

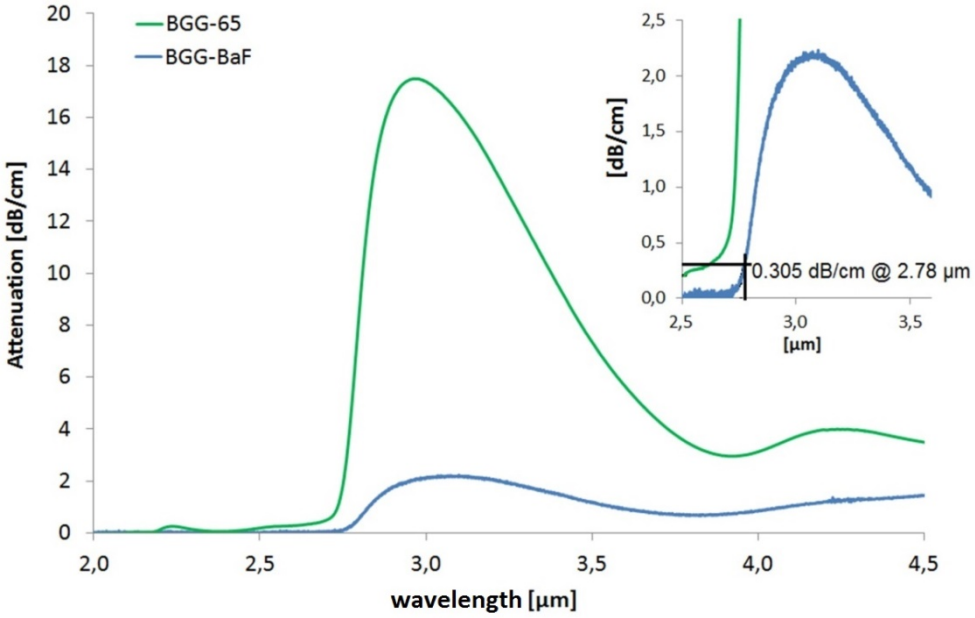

Fig. 1. Attenuation spectrum of purified (BGG-BaF), and un-purified (BGG-65) 4 mm thick BGG samples with a molecular % composition of 17.5 BaO, 65 GeO_2, 17.5 Ga_2O_3.

Waveguides were inscribed in bulk glass using a chirped pulse amplification system (Coherent RegA), operated at a repetition rate of 250 kHz and at a wavelength of 795 nm. Pulses of 70 fs (FWHM) were focused 150 µm beneath the surface of the glass sample using a 50X microscope objective (Nikon, f = 4 mm, 0.55 NA). The inscription depth was chosen to minimize the spherical aberration arising from the air-glass interface (n_{BGG65} = 1.68 @ 800 nm). A quarter-wave plate was inserted in the beam path and adjusted to produce circularly polarized light. Glass samples were translated in a direction perpendicular to the laser beam, at speeds v_x ranging from 0.05 to 50 $mm \cdot s^{-1}$, using motorized mechanical stages (Newport XML210 and GTS30V). A cylindrical lens telescope was used to produce an astigmatic beam (ellipticity of a/b = 1/8) and shape the focal volume so as to form waveguides with circular cross sections [14]. The photo-induced plasma was imaged using a 50X objective (Mitutoyo, f = 4 mm, 0.5 NA) mounted on a tube lens and a CCD camera. The size of the photo-induced plasma volume was evaluated to 5.3 µm ($2w_y$) by 7.4 µm ($2z_{Rx}$) by 1 µm ($2w_x$). The ratio between the long axis and short axis of the waveguides cross section ranges between 1.15 and 1.65 depending on exposure conditions.

After the inscription process, the end faces of the samples were cut and polished. To measure the photo-induced refractive index variations, structures were examined using a

Optical Materials EXPRESS

bright field microscope (Olympus IX71) and a camera equipped with a bi-dimensional Hartmann grating (Phasics SID4Bio). The camera is a wave-front analyser that uses lateral shearing interferometry and quantifies the accumulated phase change experienced by light transmitted through a transparent object [15]. Assuming a homogeneous refractive index change, the refractive index measured at the center of the waveguide can be obtained by dividing the accumulated phase (OPD optical path difference) by its thickness. Since incoherent white light was used in a Köhler illumination scheme, the refractive index measurement corresponds to a spectral average over the visible range.

Propagation losses of the waveguides at different wavelengths were measured using the set-up depicted in Fig. 2.

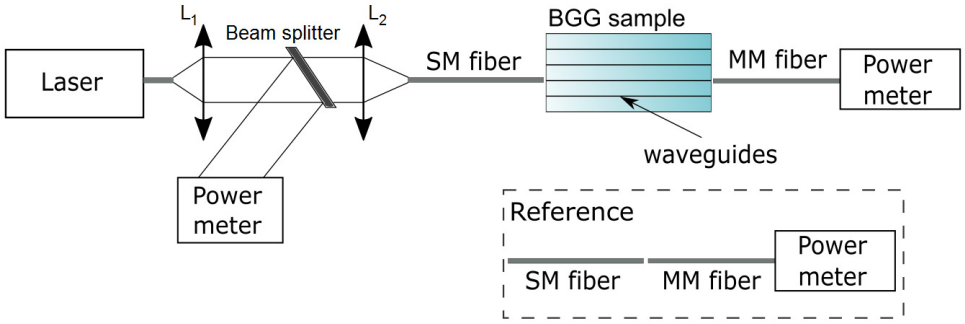

Fig. 2. Schematic of the transmission loss measurement setup.

Laser diodes emitting at 520 and 1550 nm as well as a CW fiber laser operating at λ = 2.785 µm [16] were used as characterization sources. Special care was taken for the mid-IR transmission measurements. Light from the fiber laser was first collimated using a ZnSe lens (f = 12.5 mm) and transmitted through a 50/50 beam splitter to monitor the output power (Gentec XLP12). Then, the beam was injected in a single mode fiber (Le Verre Fluoré ND7, core diameter = 14.8 µm, NA = 0.12) using another ZnSe lens (f = 25 mm) and butt-coupled to the waveguides employing 3-axis stages (Thorlabs MAX313D). The signal was collected at the other endface by a multimode fiber (Le Verre Fluoré, MM110, core diameter = 110 µm, NA = 0.22) and directed to a thermopile detector (Gentec XLP12).

In the case of visible and NIR transmission measurements, power monitoring of the source was bypassed and light from the single mode fiber (Thorlabs SM460 and Corning smf-28) of the pigtailed laser diodes (Quantum photonics QFLD-520-10S and Thorlabs SLD1550S-A1) was coupled directly to the waveguides. Light was collected using the same multimode fiber in both cases (Thorlabs GIF-62.5) and power was measured using a photodetector (Newport 818-VIS and 818-IR). For every measurement the same methodology was applied, a reference was first taken by butt-coupling the input single mode fiber to the multimode output fiber directly. Then, the BGG glass chip was inserted between the fibers and the transmitted power was optimized. Another reference was taken after the measurements as an additional validation step.

In order to image the near-field intensity profile at the output of the waveguides, the multimode fiber and the power meter were removed and replaced with a 50X objective (Olympus U-PLFLN, f = 4.5 mm, NA = 0.55) and cameras. CCD and CMOS cameras were used for visible (IDS UI-3260CP2) and near-infrared light (Point Grey Firefly MV) respectively. To obtain the intensity profile in the mid-IR, light exiting the waveguide was projected on a white screen and imaged using a thermal infrared camera (Telops TS-IR MW).

Optical Materials EXPRESS

3. Results

3.1 Photosensitivity of nominal BGG glass

A sample with the nominal BGG composition (12.5 BaO, 75 GeO_2, 12.5 Ga_2O_3, identified as BGG-75 for the remainder of the text) was irradiated by femtosecond pulses. Permanent modifications in optical material induced by the absorption of femtosecond pulses can be classified under three distinct types [17]. Type I modifications are induced using low energy pulses and characterized by a smooth and homogenous refractive index change which are favored to form optical waveguides. Type II modifications consist in birefringent structures associated with the formation of periodic nanostructures. Type III modifications are induced at higher pulse energy and are generally unsuitable for waveguiding applications. To assess the response of BGG glass to fs pulses over a wide range of exposure conditions, translation speed was varied over four orders of magnitude (0.05 to 50 $mm \cdot s^{-1}$) and pulse energy from the minimum measurable output power of the laser up to the maximum available (mean power of 1.5 W @ 250 kHz). Resulting traces were examined under a microscope. The pulse energy – translation speed window for the formation of type I and type III modifications as well as the longitudinal images of traces are presented in Fig. 3. Note that type II modifications may be formed for pulse energies close to the onset of type III modifications but were not observed during our experiment.

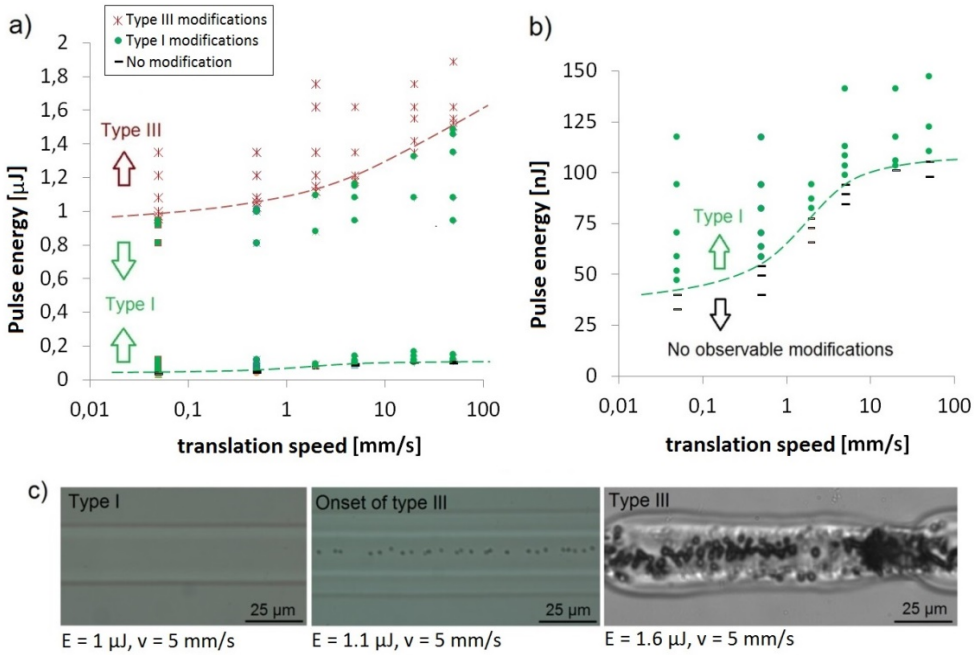

Fig. 3. a) Pulse energy vs translation speed map showing the formation of type I and type III modifications in BGG-75. b) Close-up of the onset of the type I modifications. c) Longitudinal images of type I and III modification traces.

One can see that the energy-speed window is relatively broad. This is advantageous for waveguide inscription as it eases optimization of the Δn and diameter through adjustment of exposure conditions.

Next, traces inscribed with exposure conditions that fall in the energy-speed window for the formation of type I modifications were examined more closely. The peak value of Δn and the diameter of selected traces were both measured and results are presented in Fig. 4.

Optical Materials EXPRESS

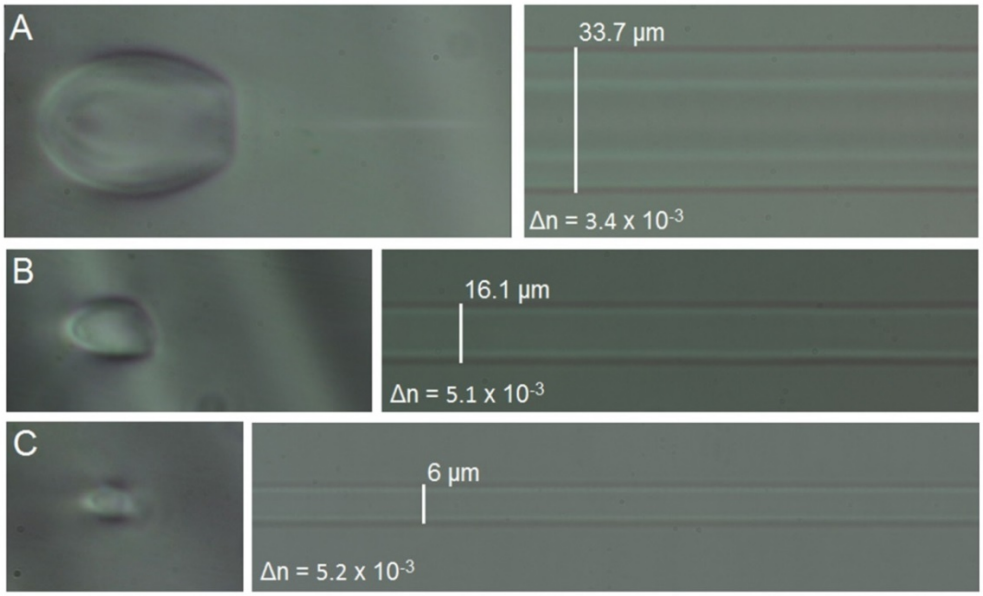

Fig. 4. Cross section (left) and longitudinal (right) images of waveguides inscribed in BGG-75. The width and the peak value of Δn is indicated. Irradiation conditions, A: E = 1 µJ, v = 0.5 mm·s^{-1}, B: E = 0.6 µJ, v = 5 mm·s^{-1}, C: E = 0.5 µJ, v = 50 mm·s^{-1}.

First we observed that the photo-induced refractive index changes are all positive and, consequently core waveguides can be inscribed over the whole range of energies and speeds investigated. The width of the waveguides grows with increased pulse energy and largely surpasses the measured plasma size of $2w_y = 5.3 \pm 0.2$ µm due to the heat accumulation effect [18]. The morphology of the waveguides is also modified as an inner core region emerges (see Fig. 4 waveguide A). This core region exhibits a lowered index change as evidenced by a dip at the center of the index profile (See Fig. 6(d) hereafter). Note that such center dip feature has been observed in other glasses prone to heat accumulation. In some cases, the small dip evolves to a large index decrease and a reversal of the sign of the index change occurs [19–21]. Since the photo-induced micro-plasma which acts as the heat source is confined to a volume of a few µm^3, the temperature falls rapidly with increasing distance from the center and as such, the induced Δn is significantly lowered as the diameter of the waveguide increases. Still, an index change larger than 5 x 10^{-3} was observed for all waveguides inscribed with pulse energy ranging between 0.3 to 0.6 µJ with low to moderate translation speeds (v_x < 50 mm·s^{-1}). A maximum Δn of 8 x 10^{-3} was measured for a waveguide inscribed with a pulse energy of 0.3 µJ and a translation speed of 5 mm·s^{-1}. The strong photo-induced Δn makes BGG glass a prime candidate for the fabrication of photonic circuits. Moreover, the thermal nature of the inscription process and the large processing window allow for the diameter to be adjusted from 5 to 35 µm while maintaining the Δn above 3 x 10^{-3}. Thus, it is in principle possible to tailor the waveguide characteristics so as to inscribe single mode waveguides operating at any wavelength over the whole transparency spectrum of the material.

3.2. Effect of germanium oxide content on the photosensitivity BGG glass

Next, we studied the influence of the relative content of germanium oxide on BGG glass response to irradiation with femtosecond pulses. Three additional samples with a different proportion of GeO_2 (maintaining a BaO/Ga_2O_3 ratio of one) were fabricated. The compositions of the samples in molar weight percentage along with the measured glass

Optical Materials EXPRESS

transition temperature T_g, crystallization temperature T_x, density ρ and linear refractive index n (at λ = 1538 nm) are presented in Table 1.

Table 1. Molar weight (%) and physical characteristics of BGG samples

Sample	BaO	GeO_2	Ga_2O_3	T_g (± 2°C)	T_x (± 2°C)	ρ [g·cm^{-3}]	n (@633nm)	n (@1538nm)
BGG-60	20	60	20	678	832	4.572	1.68	1.695
BGG-65	17.5	65	17.5	664	844	4.512	1.676	1.689
BGG-75	12.5	75	12.5	650	—	4.235	1.646	1.66
BGG-85	7.5	85	7.5	617	—	4.264	1.648	1.662

All four glass samples present similar physical characteristics. The transition temperature is relatively high which indicates a rigid glass structure. Glasses are thermally stable (T_x - T_g > 150 °C) and present a high density and a refractive index considerably lower than other mid-IR optical materials such as chalcogenides, heavy-metal oxides and crystals. Waveguides were inscribed in the four samples while varying pulse energy for three different translation speeds (0.5, 5 and 50 mm·s^{-1}). The width and Δn of the waveguides were measured and results are presented in Fig. 5.

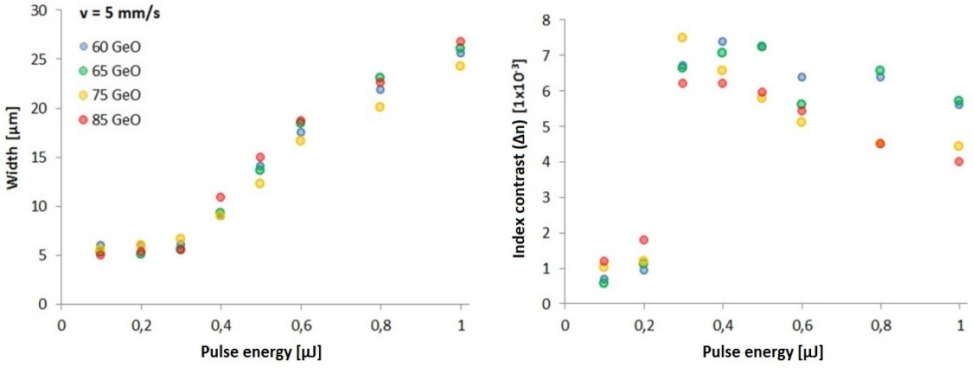

Fig. 5. Width (left) and peak Δn (right) of waveguides inscribed in BGG samples as function of pulse energy at a moderate translation speed of 5 mm·s^{-1}.

Overall, all four glass samples exhibit a remarkably similar response to irradiation with femtosecond pulses. The size of the waveguides as function of pulse energy is nearly identical for all samples. Exposure results in an increase of the refractive index in all cases but samples with a lower relative content of GeO_2 (BGG-60 and BGG-65) present a marginally stronger Δn. It is interesting to note that the refractive index change increases sharply (especially at relatively slow scan speed) for a pulse energy near 0.3 – 0.4 µJ, just as the waveguide diameter starts to grow beyond the focal volume, i.e. as heat accumulation is initiated. A further increase of pulse energy results in the formation of larger waveguides that exhibit a lessening Δn. Still, the Δn is relatively high and remains above 4 x 10^{-3} for large waveguides formed at high energy. A maximum Δn of 10.2 x 10^{-3} is reached for a waveguide inscribed in BGG-65 with a pulse energy of 0.2 µJ and a translation speed of 0.5 mm·s^{-1} (not shown in Fig. 5). It is shown that smooth high-NA (up to 0.18) waveguides with a diameter ranging between 4 and 35 µm can be formed in BGG glasses using a single pass of the laser beam. The strong photosensitivity of BGG glass to femtosecond pulses is maintained in samples with different compositions.

A last experiment was conducted using a BGG-65 sample to attempt to induce a further increase of the Δn within the boundaries of the energy-speed window for the formation of type I modification. Traces were now inscribed using several passes of the laser beam.

Optical Materials EXPRESS

Afterward, waveguides were examined and the index change was assessed. The Δn at the center of the waveguides are plotted against the number of passes in Fig. 6.

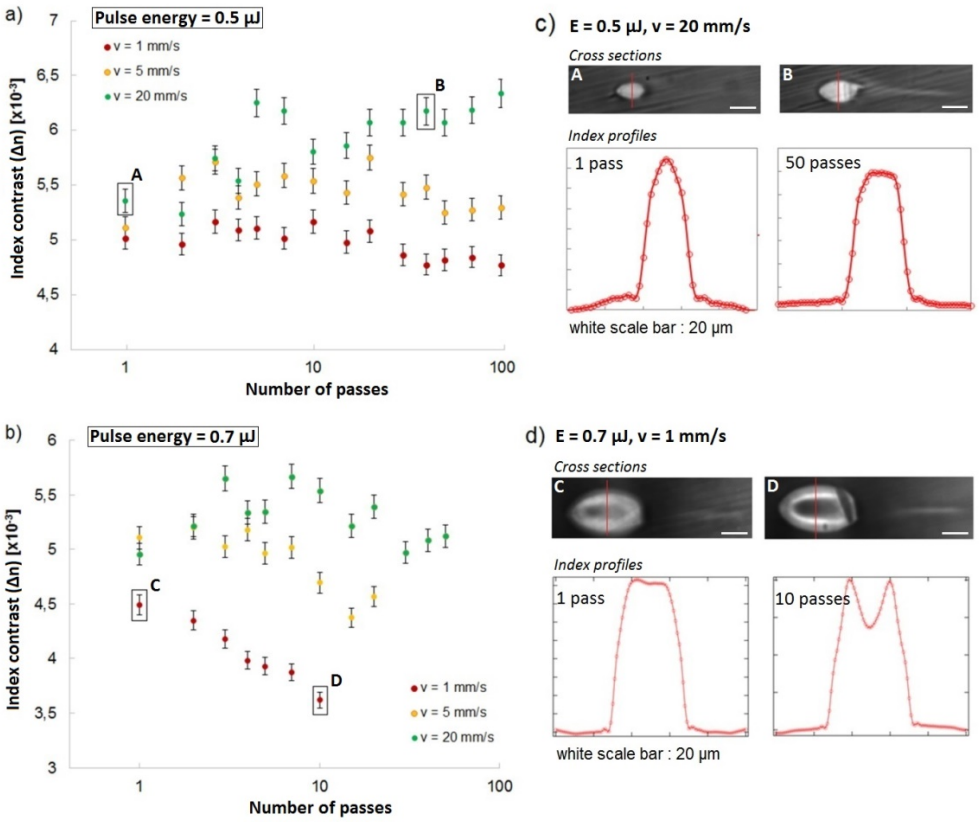

Fig. 6. Index contrast (Δn) measured at the center of waveguides inscribed in BGG-65 with a pulse energy of a) 0.5 µJ and b) 0.7 µJ as a function of the number of passes. Image of the cross section and refractive index profile of waveguides inscribed with low and high number of pulses for traces inscribed at: c) low fluence(E = 0.5 µJ, v = 20 mm·s^{-1}) and d) high fluence (E = 0.7 µJ, v = 1 mm·s^{-1}).

It is observed that successive passes of the beam do not result in a significant increase of the Δn. The sole exception is waveguides inscribed at low pulse energy (E = 0.5 µJ) and high speed (v_x = 50 mm·s^{-1}) that exhibit a modest increase of the Δn from 5.4 to 6.3 x 10^{-3} while going from a single to a hundred passes. In all other cases, the Δn remains more or less the same or even decrease for an increasing number of passes. For a small number of passes the index profile is akin to a Gaussian or flat-top curve. The morphology of the index changes evolves with increasing passes in a fashion similar to increasing fluence. For a large number of passes, a core region is formed and a strong dip of the index is observed at the center of the waveguides. One can see that the Δn saturates rapidly to its maximal value at relatively low fluence and that a further increase results in a modification of the index change spatial distribution.

3.3. Inscription of low-loss single mode waveguides for the mid-IR

Next, a glass sample with a composition similar to the previous BGG-65 sample was prepared and purified following the procedure described in the experimental methods. A significant decrease of absorption in the OH band is observed for the purified glass sample (see Fig. 1).

Optical Materials EXPRESS

Indeed, the O-H peak absorption decreases from 17.4 to 2.2 dB/cm. The authors believe that the absorption could be decreased further by optimizing the purification process.

Next, traces were inscribed in BGG-BaF sample at a translation speed ranging between 1 and 20 mm·s^{-1} and pulse energies varying between 0.5 and 0.75 µJ, which corresponds to the energy-speed window where type I waveguides with a diameter ranging from 15 to 25 µm are formed in BGG-65 glass. Again, a smooth homogenous increase of the index is observed. The photo-induced Δn in BGG-BaF decreases considerably compared to the Δn induced in un-purified samples. Actually, the Δn is kept between 2.2 and 3.0 x 10^{-3} over the range of investigated exposure conditions. In order to increase the index contrast, waveguides were inscribed using successive laser passes at the same position in the sample and a similar response is observed for the purified glass compared to the other sample. Thus, it is not possible to increase the Δn beyond ~3 x 10^{-3} even when exposing the glass sample to a large number of passes. Our results show that the purification process can considerably affect the photosensitivity of the prepared glass. Here, enhanced transmission of the glass in the mid-IR is gained at the expense of a smaller achievable index contrast.

Nevertheless, the Δn is still sufficiently strong to allow for the formation of waveguides which match the characteristics of a common mid-IR single mode optical fiber (NA = 0.08-015, core diameter = 12-18 µm). This is a requirement for the integration of embedded photo-induced photonic devices in optical systems. Exposure conditions were adjusted finely to yield the formation of 16 mm long waveguides in BGG-BaF glass designed for single mode operation at the central wavelength of the mid-IR fiber laser. Images of the longitudinal and cross section of the resulting waveguide are presented in Fig. 7.

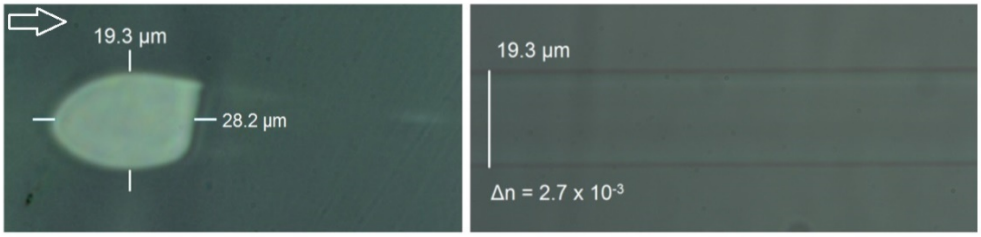

Fig. 7. Cross section (left) and longitudinal (right) images of a waveguide inscribed in BGG-BaF glass (E = 0.65 µJ, v = 5mm·s^{-1}). The white arrow indicates the beam direction during the inscription process.

The waveguide shown in Fig. 7 presents a Δn of 2.7 x 10^{-3} (NA = 0.09) and transverse dimensions of 19.3 µm by 28.2 µm. In order to assess the optical performances of the waveguides, λ = 515, 1550 and 2780 nm light was injected in the waveguide and the transmission as well as the near-field intensity profile were measured. Images of guided mode at each wavelength and the insertion loss of the optimized waveguide are presented in Fig. 8.

Optical Materials EXPRESS

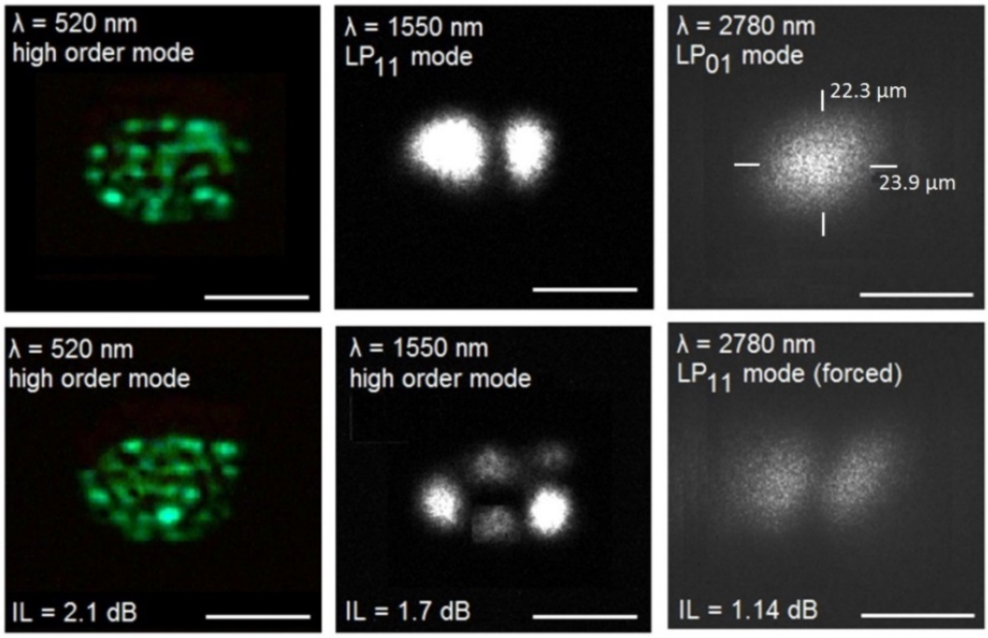

Fig. 8. Near field intensity profile of light at different wavelengths transmitted through the waveguide. The white scale bar equals 20 µm.

As expected, the waveguide supports the propagation of only two LP modes at λ = 2.78 µm. Indeed, if light is injected in the center of the waveguide only the fundamental mode is guided whereas propagation of the LP_{11} mode can be forced if the injection beam is slightly offset toward the edge of the waveguide.

A total insertion loss of 1.14 dB was measured using the procedure described in section 2. By taking into account power loss of 0.55 dB originating from the Fresnel reflections (n = 1.672 @ 2.78 µm), the sum of the coupling and propagation losses is evaluated at 0.59 dB. Since the waveguide is 1.6 cm long, the propagation loss corresponds to 0.37 dB/cm or less depending on the magnitude of the coupling loss.

The small fraction of the incident light that is not coupled to the waveguides but propagates in pristine bulk glass may be collected by the large multimode fiber. A basic beam propagation calculation was performed to estimate the contribution of guided and unguided light to the total power measured at the output of the fiber. An upper bound for the propagation losses of 0.5 ± 0.1 dB/cm was determined. This value is slightly lower than the best result (0.65 dB/cm) reported for mid-IR waveguides based on a refractive index increase [13].

Insertion losses of 2.1 and 1.7 dB are measured for light propagating at λ = 520 and 1550 nm respectively. This is caused by the multimode operation of the waveguide at these wavelengths since higher order modes leak more easily and generally experience higher propagation losses.

3. Conclusion

We presented an extensive study of buried waveguides inscription in BGG glass using a femtosecond laser. Smooth type I modifications can be inscribed using a relatively wide range of exposure conditions. Thus, waveguides with diameters ranging from 4 to 35 µm and index change up to 10.2 x 10^{-3} can be formed by varying pulse energy and translation speed. The photo-induced modification results in an increase of the refractive index over the whole range or exposure conditions tested. It is seen that the heat accumulation effect plays a key role in

Optical Materials EXPRESS

the modification process, as a sharp increase of the index change coincides with the onset of the thermal regime. Exposure under high fluence or using a large number of successive passes of the laser beam results in the formation of a core region with a central dip. Samples with a different relative content of germanium dioxide were irradiated and only a few slight differences in the response to fs pulses are reported. A sample with a composition akin to nominal BGG (17.5 BaO, 65 GeO_2, 17.5 Ga_2O_3) was fabricated and underwent a purification process in order to eliminate bound hydroxyl. Consequently, transmission in the mid-IR was significantly enhanced but the photosensitivity to femtosecond pulses was lessened as the maximum induced index contrast dropped to 3 x 10^{-3}. Improvement over the fabrication process and modification to the BGG glass composition should allow enhancing the transmission in the infrared while preserving the strong photosensitivity. Still, the Δn induced in the purified sample is sufficiently strong to allow for the formation of waveguides which precisely match the optical characteristics of standard mid-IR single mode optical fibers. Careful adjustment of the exposure conditions allowed for the inscription of single mode waveguides operating at a wavelength of 2.78 µm. Low propagation losses of 0.5 dB/cm are reported. Our results clearly demonstrate the potential of BGG glasses as ideal candidates for the development of embedded photonic devices operating in the 2-4 µm spectral window.

Funding

Natural Sciences and Engineering Research Council of Canada (NSERC) (IRCPJ469414-13); Canada Foundation for Innovation (CFI) (37422); French National Research Agency (ANR), in the framework of the "Investments for the Future" (LAPHIA ANR - n ° ANR-10-IDEX-03-02).

Acknowledgement

The authors wish to thank Samuel Gouin and Yasmine Alikacem.